The Journal of Infectious Diseases

MAJOR ARTICLE

Airborne SARS-CoV-2 Is Rapidly Inactivated by Simulated Sunlight

Michael Schuit, Shanna Ratnesar-Shumate, Jason Yolitz, Gregory Williams, Wade Weaver, Brian Green, David Miller, Melissa Krause, Katie Beck, Stewart Wood, Brian Holland, Jordan Bohannon, Denise Freeburger, Idris Hooper, Jennifer Biryukov, Louis A. Altamura, Victoria Wahl, Michael Hevey, and Paul Dabisch

National Biodefense Analysis and Countermeasures Center, Operated by Battelle National Biodefense Institute for the US Department of Homeland Security Science and Technology Directorate, Frederick, Maryland, USA

(See the Major Article by Ratnesar-Shumate et al., on pages 214–22.)

Aerosols represent a potential transmission route of COVID-19. This study examined effect of simulated sunlight, relative humidity, and suspension matrix on stability of SARS-CoV-2 in aerosols. Simulated sunlight and matrix significantly affected decay rate of the virus. Relative humidity alone did not affect the decay rate; however, minor interactions between relative humidity and other factors were observed. Mean decay rates (± SD) in simulated saliva, under simulated sunlight levels representative of late winter/early fall and summer were 0.121 ± 0.017 min^{-1} (90% loss, 19 minutes) and 0.306 ± 0.097 min^{-1} (90% loss, 8 minutes), respectively. Mean decay rate without simulated sunlight across all relative humidity levels was 0.008 ± 0.011 min^{-1} (90% loss, 286 minutes). These results suggest that the potential for aerosol transmission of SARS-CoV-2 may be dependent on environmental conditions, particularly sunlight. These data may be useful to inform mitigation strategies to minimize the potential for aerosol transmission.

Keywords. SARS-CoV-2; COVID-19; aerosol decay; aerosol persistence; sunlight; relative humidity.

Severe acute respiratory syndrome coronavirus 2 (SARS-CoV-2) causes the disease COVID-19, an acute respiratory disease characterized by fever, dry cough, shortness of breath, and pneumonia. Multiple routes of exposure are potentially relevant, but uncertainty remains regarding the relative contributions of these various routes to disease transmission [1]. In previous outbreaks with related coronaviruses, including severe acute respiratory syndrome coronavirus 1 (SARS-CoV-1) and Middle East respiratory syndrome coronavirus (MERS-CoV), both genetic material and infectious virus were detected in air samples, suggesting aerosol transmission as a possible transmission route [2–5]. Similarly, SARS-CoV-2 genetic material has been detected in air samples taken in COVID-19 patient treatment facilities, as well as in surface swabs from room exhaust vents and patient masks, suggesting the possibility of aerosol transmission [6–8].

Aerosol generation from the respiratory tract is known to occur during coughing, sneezing, talking, and breathing [9, 10]. Leung et al demonstrated that the genetic material of the coronaviruses NL63, OC43, and HKU1 could be detected in aerosols collected from the exhaled breath of infected individuals [11]. While no data exist on the viral load of SARS-CoV-2 in exhaled breath of infected individuals, high loads of SARS-CoV-2 genomic material have been detected in upper respiratory tract specimens of infected patients in throat and nasal swabs [12, 13]. The virus has also been detected by reverse transcription polymerase chain reaction (RT-PCR) in bronchoalveolar lavage, fibrobronchoscope brush biopsy, sputum, and pharyngeal swabs [14]. Therefore, it is plausible that aerosols containing SARS-CoV-2 could be generated from the respiratory tract of infected individuals. Additionally, previous studies have demonstrated that certain medical procedures have the potential to generate aerosols and, therefore, represent an additional potential source of infectious aerosols in clinical settings [15, 16].

For aerosol transmission to occur, viruses within aerosol particles must remain infectious between generation and inhalation by a susceptible host. Loss of infectivity during this period will decrease the likelihood of aerosol transmission. van Doremalen et al [17] have reported that SARS-CoV-2 is detectable in aerosols for several hours in darkness at room temperature. Similar results have been reported previously for other coronaviruses under similar conditions [18, 19]. Environmental conditions, including relative humidity and sunlight, have been shown to influence the decay rate of infectious viruses in aerosols [18, 20–24]. However, no such data on the influence of these factors on the aerosol persistence of SARS-CoV-2 exist. Therefore, the present study examined the influence of both simulated sunlight and relative humidity on the stability of SARS-CoV-2 in aerosols

Received 4 May 2020; editorial decision 5 June 2020; accepted 8 June 2020; published online June 11, 2020.

Correspondence: Paul Dabisch, PhD, National Biodefense Analysis and Countermeasures Center, 8300 Research Plaza, Frederick, MD 21702 (paul.dabisch@nbacc.dhs.gov).

The Journal of Infectious Diseases® 2020;222:564–71

DOI: 10.1093/infdis/jiaa334

generated from virus suspended in different liquid matrices. The data generated will further our understanding of factors that have the potential to influence aerosol transmission of SARS-CoV-2 and could be utilized to inform mitigation strategies for aerosol transmission of virus during the current pandemic.

METHODS

Cells

Vero Cells (ATCC CCL-81) were grown at 37°C and 5% CO_2 in culture medium, consisting of minimum essential medium (Gibco) supplemented with 10% heat-inactivated fetal bovine serum (Hyclone or Atlanta Biologicals), 2 mM GlutaMAX (Gibco), 0.1 mM nonessential amino acids solution (Gibco), 1 mM sodium pyruvate (Gibco), and 1% antibiotic-antimycotic solution (Gibco).

Virus

A passage 4 isolate of SARS-CoV-2 (BetaCoV/USA/WA1/2020) was obtained from BEI resources and passaged twice in Vero cells to produce a stock of virus that was concentrated by tangential flow filtration and frozen at −80°C until use. For aerosol tests, aliquots of the concentrated virus were thawed and diluted 1:10 in either fresh culture medium or simulated saliva, formulated as described in the ASTM standard for measuring virus decontamination efficacy [25], but prepared with KH_2PO_4 and K_2HPO_4 at final concentrations of 15.4 mM and 24.6 mM, respectively. Diluted virus aliquots were prepared daily from frozen stocks and kept on ice between tests. Titers of infectious virus in aerosol samples were determined by microtitration assay on confluent monolayers of Vero cells in 96-well plates. Plates were incubated at 37°C and 5% CO_2, with cytopathic effect read 4 days post infection and viral titers calculated according to the method of Kärber and Spearman [26, 27]. The pH and solids content of viral suspensions diluted in each matrix was measured in triplicate using a SevenExcellence pH meter (Mettler-Toledo) and MA35 Moisture Analyzer (Sartorius AG), respectively. Protein content was quantified using a Pierce BCA Protein Assay Kit (Thermo Fisher Scientific) with an albumin standard curve. The assay was read on a SpectraMax M5 plate reader (Molecular Devices).

Test Systems

Two different environmentally controlled rotating drum aerosol chambers, with volumes of 16 L and 208 L, were used in the present study to expose aerosols containing SARS-CoV-2 to controlled levels of temperature, relative humidity, and simulated sunlight. The environmental control systems were similar for both drums, and have been described previously for 1 of these drums [21]. Briefly, the temperature of the air inside the drum was regulated by a temperature-controlled glycol solution circulated through channels in the walls of the drums. Relative humidity was controlled by adjusting the balance of dry and humid air entering the drum prior to tests, during filling, and as makeup air when aerosol samples were collected from the drums. Temperature and relative humidity probes in the interior of each drum were used to record the values of these parameters in 10-second intervals over the course of each test. For each test, the mean and standard deviation were determined for these parameters using data from the beginning of the first aerosol sample to the end of the final sample.

For a subset of tests, SARS-CoV-2 aerosols were exposed to simulated sunlight generated by a solar simulator (Newport Oriel) equipped with a 320-nm highpass filter (WG320 filter PN SL07614; Solar Light Co.) through a fused-silica window on 1 face of the chambers. Tests were conducted at 1 of 2 intensity levels, with spectra designed to represent the ultraviolet (UV) range (280–400 nm) of natural sunlight. The 2 spectra used in the present study, referred to hereafter as high-intensity and mid-intensity, have similar UV irradiances to model spectra from the National Center for Atmospheric Research's (NCAR) tropospheric ultraviolet and visible (TUV) radiation model for midday sunlight on a clear day at sea level at 40°N latitude in either mid-June or early March/October, respectively. Spectra produced by the solar simulator were measured immediately outside of the chamber window using a spectroradiometer (OL756; Gooch & Housego) equipped with a 2-inch (5.08-cm) diameter integrating sphere light receptor (IS-270; Gooch & Housego), and corrected for transmission losses through the fused-silica window. Representative spectra from the solar simulator and comparisons to model spectra from NCAR's TUV radiation model in the UVA and UVB ranges are shown in Figure 1. Model spectra were calculated for noon on 7 March, 4 October, and 21 June at 40°N latitude using default input parameters for atmospheric conditions, elevation, and surface albedo. Integrated irradiances for the UVA and UVB portions of the spectra for both the measured and TUV model spectra demonstrate close agreement between the measured and model values (high intensity, 1.91 W/m^2 UVB measured vs 1.84 W/m^2 UVB predicted by TUV for 21 June; midintensity, 0.94 W/m^2 UVB measured vs 0.92 W/m^2 UVB predicted by TUV for 7 March and 4 October). No irradiance was detectable above the background level measured in darkness for wavelengths less than approximately 295 nm.

Aerosol Decay Tests

Virus-containing aerosol particles of respiratory origin have been found in a range of particle sizes from submicron to several microns in diameter [10, 28, 29]. In the present study, the target mass median aerodynamic diameter (MMAD) was 2 μm, an approximate midpoint of the range of relevant possible sizes. Aerosols were generated into an external stainless steel plenum attached to each drum using an air assist nozzle (IAZA5200415K; Lee Company). The nozzle was supplied with

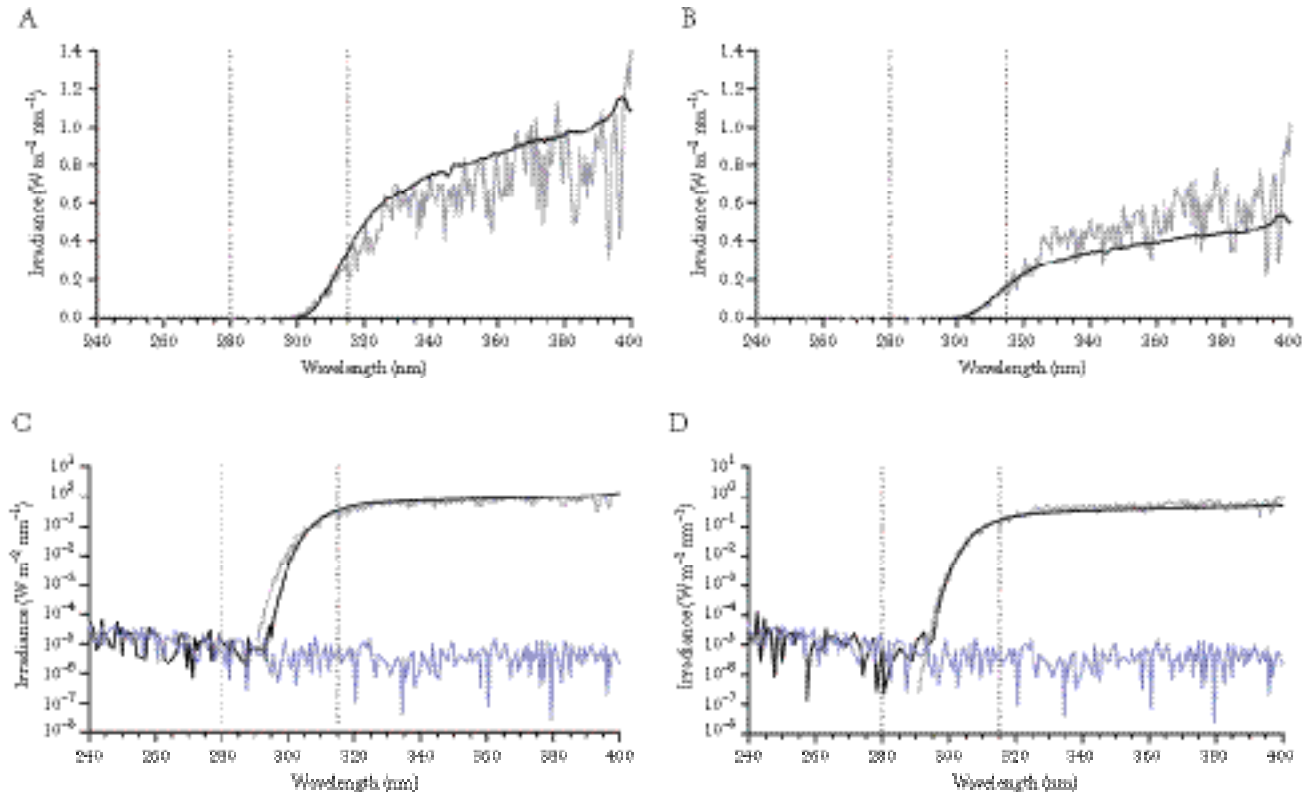

Figure 1. Representative spectra for simulated sunlight. Simulated sunlight spectra utilized in the present study (black lines), spectra from the National Center for Atmospheric Research (NCAR) tropospheric ultraviolet and visible (TUV) radiation model for noon at 40°N latitude at sea level (gray lines), and spectra measured for darkness (blue lines) are shown (for color figure refer online version). *A*, Spectra for high-intensity simulated sunlight and TUV model for 21 June. *B*, Spectra for midintensity simulated sunlight and TUV model for both 7 March and 4 October. *C*, Spectra for high-intensity simulated sunlight and TUV model for 21 June, with irradiance plotted logarithmically. *D*, Spectra for midintensity simulated sunlight and TUV model for both 7 March and 4 October, with irradiance plotted logarithmically. Integrated irradiances for the UVA and UVB portions of the spectra for both the measured and TUV model spectra demonstrate close agreement between the measured and model values. For high-intensity simulated sunlight, measured integrated UVB irradiance was 1.91 W/m^2 vs 1.84 W/m^2 predicted by TUV for 21 June. Measured integrated UVA irradiance was 69.76 W/m^2 vs 58.50 W/m^2 predicted by TUV for 21 June. For midintensity simulated sunlight, measured integrated UVB irradiance was 0.94 W/m^2 vs 0.92 W/m^2 predicted by TUV for 7 March and 4 October. Measured integrated UVA irradiance was 31.97 W/m^2 vs 40.54 and 40.25 W/m^2 predicted by TUV for 7 March and 4 October, respectively. No irradiance was detectable above the background of the spectroradiometer measured in darkness for wavelengths less than approximately 295 nm. Vertical dashed lines represent the cutoffs between UVC and UVB (280 nm), and UVB and UVA (315 nm).

dry, compressed air at 45 psig (310 kPA) and supplied with the viral suspension at 200 to 300 μL/min using a syringe pump.

Aerosol was drawn from the external plenum into the drums. The filling time differed for the 2 drums due to the difference in volume and was 30 seconds for the smaller drum and 60 seconds for the larger drum. Following filling, aerosols were allowed to mix in the drum for 30 seconds prior to collection of the first sample. Aerosols were then aged in the drums for up to 60 minutes. Five samples of the aerosol present in a drum were collected over the course of each test. The test duration and sample intervals were determined based on the anticipated decay rate for a given set of environmental conditions. At each sampling time point, a 10-second sample was collected using an aerodynamic particle sizer (APS; model 3321; TSI Inc.) to measure the mass concentration and size distribution of the aerosol in the drum. Immediately following the APS sample, a 20 to 60-second sample was collected onto a 25-mm gelatin filter (PN 225–9551; SKC, Inc.) in a Delrin filter holder (PN 1109; Pall Corporation) operated at 5 L/min. The gelatin filter was immediately removed from the holder and dissolved in 10 mL of culture medium to resuspend the collected virus. Relative humidity-conditioned makeup air entered the drum during both APS and gelatin filter sampling to maintain the relative humidity and neutral pressure in the chamber.

Tests were conducted in both suspension matrices across a range of relative humidity levels (20%, 45%, and 70%) and simulated sunlight intensities (darkness, midintensity, and high intensity). A 2×2 full factorial design with a center-point was utilized to examine the effect of each parameter, as well as interactions between parameters, on the decay rate of aerosolized SARS-CoV-2. Tests were conducted at all combinations of the low and high levels of both factors, as well as at the midpoint levels of both factors. This experimental design is an efficient approach that allows examination of the impact of relative humidity and simulated sunlight, as well as potential interactions of these factors, while minimizing the total number of tests

required. Additional tests were conducted without simulated sunlight at target relative humidity values of 37% and 53% to examine the effect of relative humidity under temperature and light conditions relevant to indoor environments in greater detail. Three to 6 replicate tests were performed for each combination of suspension matrix and environmental condition. All tests were conducted at a target temperature of 20°C.

Data Analysis

The aerosol concentration of infectious SARS-CoV-2 within the drum at each time point, in median tissue culture infectious dose/L ($TCID_{50}$/L) air, was calculated as the total amount of virus collected by the gelatin filter divided by the amount of air sampled. The aerosol mass concentration within the drum at each time point, in mg/m^3, was calculated from the data collected by the APS. For each test, time-series $\log_{10}$ transformed viral and mass aerosol concentration data were fit using linear regression in Microsoft Excel, version 2016. The slopes of these regression lines represent the decay rates of infectious virus and total aerosol mass in the chamber, respectively. In the published literature, decay is often reported as the decay constant from a 1-phase exponential fit [18, 21, 30–33]. To allow a direct comparison to these values, the slope was converted from log base 10 to log base *e*, as this value is equivalent to the decay constant from a 1-phase exponential decay fit of the data.

The decay constant associated with viral aerosol concentrations measured with the filter samplers (k_{Filter}) reflects decreases in concentration due both to losses in viral infectivity and to physical losses of aerosol, including settling on chamber surfaces and removal of material during sampling. To isolate losses in viral infectivity and determine a decay constant for infectivity ($k_{Infectivity}$), the decay constant associated with the mass concentration ($k_{Physical}$), which reflects only physical losses specific to the test system and experimental protocol, was subtracted from k_{Filter}.

Fifty-nine total tests were performed across all combinations of suspension matrix and environmental conditions. Three tests were not utilized in subsequent analyses due to poor linear regression fits of the time-series viral aerosol concentration data, as quantified by coefficients of determination (r^2) values less than 0.70 and a root mean square error greater than 0.3. A minimum of 3 replicate tests were performed for each combination of temperature, humidity, and simulated sunlight tested.

Regression analysis was utilized to assess the influence of simulated sunlight, relative humidity, and suspension matrix on $k_{Infectivity}$. A full factorial model including interactions between the 3 factors was initially assumed. Stepwise regression was used to identify and remove predictors that were insignificant using a backward elimination approach (JMP 11.2.0; SAS Institute). Minimization of the Akaike information criterion was used as the stopping rule. The mean relative humidity from each individual test and the integrated UVB irradiance measured for high and midintensity simulated sunlight were used in the model. Environmental parameters used in the model were standardized by transformation to a range spanning −1 to +1, to allow direct comparison of the parameter estimates from the regression model. All values are presented as arithmetic mean ± standard deviation unless otherwise noted.

RESULTS

Concentrated SARS-CoV-2 viral suspensions were diluted in either simulated saliva or culture medium. Virus diluted into simulated saliva had a solids content of 1.31% ± 0.03%, a pH of 7.4 ± 0.0, and protein concentration of 3.58 ± 0.07 mg/mL. Simulated saliva without virus had a solids content of 1.01% ± 0.10%, a pH of 7.3, and protein concentration of 0.68 ± 0.00 mg/mL. Virus diluted into culture medium had a solids content of 1.71% ± 0.03%, a pH of 7.4, and protein concentration of 6.77 ± 0.03 mg/mL. Culture medium without virus had a solids content of 1.53% ± 0.07%, a pH of 7.1, and protein concentration of 4.46 ± 0.14 mg/mL.

For aerosol decay testing with target relative humidity levels of 20%, 37%, 45%, 53%, and 70%, the mean relative humidity values (± SD) were 20.1% ± 2.2%, 38.0% ± 1.7%, 43.6% ± 1.4%, 52.8% ± 0.6%, and 69.0% ± 2.5%, respectively. The mean temperature across all tests was 20.1°C ± 0.3.

The mean MMAD and geometric standard deviation (GSD) at the first sample collected across all tests in simulated saliva were 1.96 ± 0.05 μm and 1.62 ± 0.04 μm, respectively. For tests in culture medium, these values were 1.98 ± 0.08 μm and 1.60 ± 0.04 μm, respectively. A small downward shift in the MMAD occurred over the course of each test due to a more rapid physical loss of larger particles in the size distribution. As a result, the mean MMAD of aerosols generated from simulated saliva and culture medium at the final sample were 1.78 ± 0.14 μm and 1.88 ± 0.13 μm, respectively.

Decay data for SARS-CoV-2 in aerosols are shown in Figure 2, Figure 3, and Table 1. Average decay constants for infectivity ranged from near zero for tests without simulated sunlight to 0.48 min^{-1}, or 38%/min, for tests with high-intensity simulated sunlight at 70% relative humidity. Stepwise regression analysis demonstrated that $k_{Infectivity}$ was dependent on the simulated sunlight intensity and the suspension matrix ($P < .0001$ and $P = .0004$, respectively), but not relative humidity ($P = .0946$). Interactions between suspension matrix and simulated sunlight intensity ($P < .0001$), suspension matrix and relative humidity ($P = .0017$), and simulated sunlight intensity and relative humidity ($P = .0463$) were also significant. While the effect of suspension matrix was statistically significant, the magnitude of the effect of simulated sunlight was much greater, as suggested by a greater standardized regression coefficient (−0.117 for

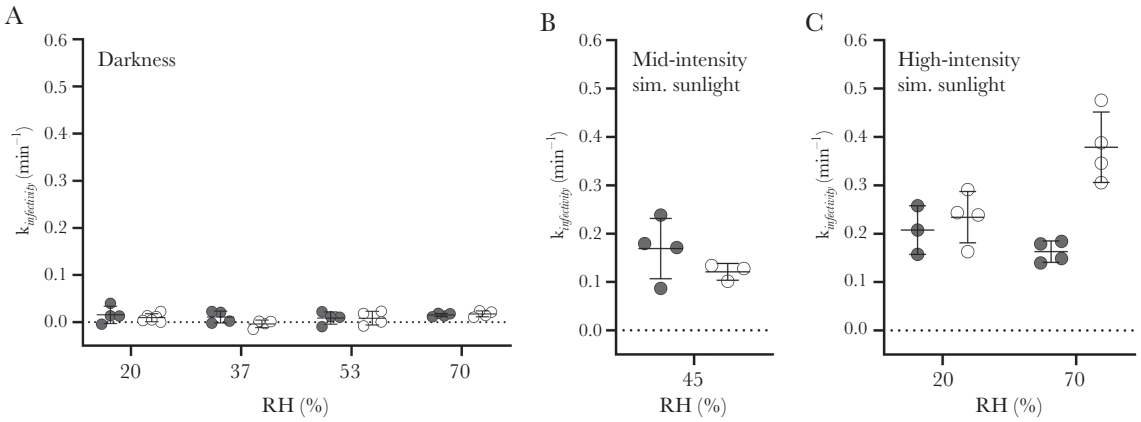

Figure 2. Aerosol decay data for SARS-CoV-2 at 20°C. Tests were conducted in darkness (*A*), at midintensity simulated (Sim.) sunlight (*B*), and at high-intensity simulated sunlight (*C*). Data from tests with the virus suspended in simulated saliva and culture medium are shown in white and grey, respectively, with bars indicating the arithmetic mean ± standard deviation of the $k_{Infectivity}$ values for each data set. $k_{Infectivity}$ was dependent on the simulated sunlight intensity and the suspension matrix ($P < .0001$ and $P = .0004$, respectively), but not relative humidity (RH).

simulated sunlight vs 0.022 for matrix). The overall adjusted r^2 for the model was 0.88.

DISCUSSION

The present study examined the influence of simulated sunlight and relative humidity on the stability of SARS-CoV-2 in aerosols generated from virus suspended in either simulated saliva or culture medium at 20°C. Simulated sunlight rapidly inactivated the virus in aerosols in either suspension matrix, with half-lives of less than 6 minutes and 90% of the virus inactivated in less than 20 minutes for all simulated sunlight levels tested. There was a small but statistically significant reduction in decay rate under high-intensity sunlight when the virus was suspended in culture medium compared to simulated saliva, suggesting that the matrix in which the virus is suspended may also be an important factor to consider when examining the persistence of SARS-CoV-2 in an aerosol. While it has been reported previously that UVC can inactivate aerosolized coronaviruses [34], the present study is the first to demonstrate that simulated sunlight, with UVA and UVB levels similar to natural sunlight, is also able to inactivate airborne coronaviruses. It should be noted that many additional factors beyond the relative stability of the virus in an aerosol contribute to the potential for aerosol transmission of disease. These include the amount of virus present in an aerosol, the size and infectious dose of aerosol particles, the distance and airflow dynamics between infected and uninfected individuals, and the presence of mitigation measures such as personal protective equipment. Therefore, while the results of the present study provide novel data regarding the stability of SARS-CoV-2 aerosols in the environment, additional data are needed to provide a comprehensive assessment of the potential for aerosol transmission.

Relative humidity alone did not significantly affect decay of the virus, although there were interactions identified between relative humidity and the other factors. However, the magnitude of these interactions was minor compared to the magnitude of the effect of simulated sunlight. The half-lives estimated from the mean decay constants across all relative humidity levels without simulated sunlight present were 55 and 86 minutes for aerosols generated from virus suspended in culture medium and simulated saliva, respectively. The half-life from the present study for culture medium is similar to the value of 1.1 hours reported recently for SARS-CoV-2 in darkness and 65% relative humidity by van Doremalen et al [17]. The prolonged persistence of SARS-CoV-2 under conditions representative of indoor environments highlights the need for additional studies to better understand the potential sources of aerosols and viral load present in these settings.

It has been previously reported that other coronaviruses were significantly less stable at higher relative humidities, with the half-life for human coronavirus 229E decreasing from 67.3 ± 8.2 hours to 3.3 ± 0.2 hours for relative humidity levels of 50% and 80%, respectively [18]. While a similar effect was not observed for SARS-CoV-2 in the present study, it is possible that the shorter test durations used in the present study precluded detection of this effect of relative humidity. It is possible that additional tests of longer duration without simulated sunlight would allow a better assessment of the effect of relative humidity on SARS-CoV-2 in aerosols, but the results of the present study suggest that any such effect would be relatively minor in comparison to the effect of sunlight.

Previous studies have also demonstrated that numerous other factors can influence the survival of microorganisms in aerosols. In particular, temperature has been shown previously to affect the survival of coronaviruses, including MERS, in aerosols [18, 19]. Furthermore, while the stability SARS-CoV-1 and SARS-CoV-2 in aerosols were shown to be similar under a single set of conditions [17], other studies have demonstrated

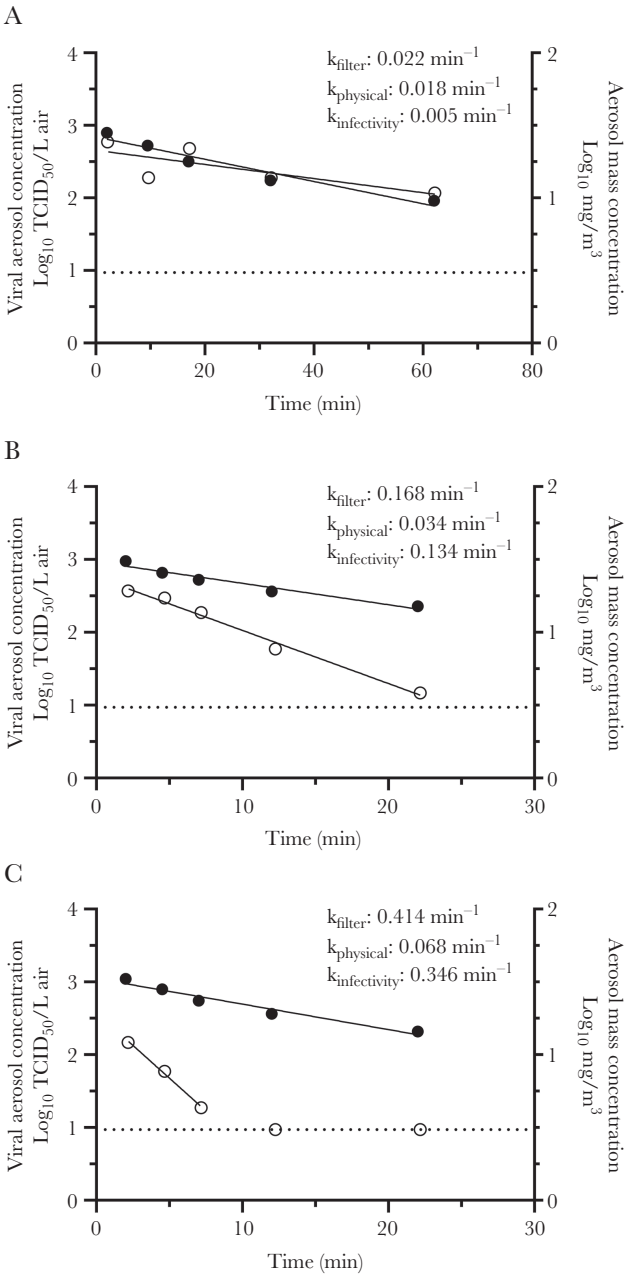

Figure 3. Representative viral and mass aerosol concentration profiles for SARS-CoV-2 in simulated saliva. Representative decay profiles and associated decay constants for both viral infectivity and aerosol mass from individual tests are shown for (*A*) no simulated sunlight at 20% relative humidity and 20°C, (*B*) midintensity simulated sunlight at 45% relative humidity and 20°C, and (*C*) high-intensity simulated sunlight at 70% relative humidity and 20°C. The decay of the aerosol mass concentration, in log_{10} mg/m^3 (black circles), was similar across the 3 tests, while the decay rate of infectious viral aerosols, in log_{10} median tissue culture infectious dose/L ($TCID_{50}$/L) air (white circles), increased as the intensity of simulated sunlight was increased. The dashed line at 0.97 log $TCID_{50}/L_{air}$ indicates the limit of detection for infectious virus; points on this line were not included in curve fits.

that the aerosol stability can vary between related viruses [35–38]. Therefore, additional testing incorporating a range of relevant temperatures and additional isolates of SARS-CoV-2 should be conducted to better estimate the range of potential decay rates associated with SARS-CoV-2.

Table 1. Summary of SARS-CoV-2 Decay at 20°C in Aerosols

Matrix	Simulated Sunlight	n	$k_{Infectivity}$, min^{-1}	Decay Rate, %/min
Simulated saliva	None	18	0.008 ± 0.011	0.8 ± 1.1
	Mid intensity	3	0.121 ± 0.017	11.4 ± 1.5
	High intensity	8	0.306 ± 0.097	26.1 ± 7.1
Culture medium	None	16	0.013 ± 0.012	1.2 ± 1.2
	Mid intensity	4	0.169 ± 0.062	15.4 ± 5.3
	High intensity	7	0.182 ± 0.041	16.6 ± 3.3

Decay constants ($k_{Infectivity}$), decay rate, and half-life calculated from the mean $k_{Infectivity}$ values are summarized as a function of matrix and simulated sunlight level. Decay constants and rates are presented as the arithmetic mean ± standard deviation of each data set. Results across different relative humidity levels were pooled because relative humidity was determined not to be a significant factor affecting decay. Data from 56 tests are included; 3 tests were not included due to poor linear regression fits of the time-series viral aerosol concentration data.

It was necessary to concentrate the viral stock used in the present study to ensure that quantifiable concentrations of virus were present in aerosols. However, the addition of the concentrated viral stock to the simulated saliva significantly altered the properties of the simulated saliva, specifically the fractional solids and protein content. Thus, while a small difference in decay was observed between the simulated saliva and culture medium in the presence of simulated sunlight, it is possible that the viral suspension diluted in simulated saliva is not representative of the composition of expelled particles in infected individuals. Previous studies have shown that particle composition can affect the decay rate of infectious viruses in aerosols [39–41]. Therefore, additional studies aimed at understanding the influence of suspension matrix composition on the survival of SARS-CoV-2 in aerosols, as well as studies examining the composition of relevant bodily fluids in infected individuals, are needed to inform matrix selection in future studies.

The present study provides the first data on the influence of relative humidity, simulated sunlight, and suspension matrix on the survival of SARS-CoV-2 in aerosols and suggests that sunlight may be an important factor influencing the risk of aerosol transmission of disease. These data, in conjunction with studies on the epidemiology of COVID-19, aerosol sampling studies in clinical settings, and studies on the infectious dose of SARS-CoV-2, may be useful to better understand the potential for this virus to spread via the aerosol route.

Notes

Disclaimer. The views and conclusions contained in this document are those of the authors and should not be interpreted as necessarily representing the official policies, either expressed or implied, of the Department of Homeland Security (DHS) or the US Government. The DHS does not endorse any products or commercial services mentioned in this presentation. In no event shall the DHS, Battelle National Biodefense Institute, or National Biodefense Analysis and Countermeasures Center have any responsibility or liability for any use, misuse, inability

to use, or reliance upon the information contained herein. In addition, no warranty of fitness for a particular purpose, merchantability, accuracy or adequacy is provided regarding the contents of this document.

Financial support. This work was supported by the DHS Science and Technology Directorate (agreement number HSHQDC-15-C-00064 awarded to Battelle National Biodefense Institute for the management and operation of the National Biodefense Analysis and Countermeasures Center, a Federally Funded Research and Development Center).

Potential conflicts of interest. All authors: No reported conflicts of interest. All authors have submitted the ICMJE Form for Disclosure of Potential Conflicts of Interest. Conflicts that the editors consider relevant to the content of the manuscript have been disclosed.

References

1. Sohrabi C, Alsafi Z, O'Neill N, et al. World Health Organization declares global emergency: A review of the 2019 novel coronavirus (COVID-19). Inter J Surg **2020**; 76:71–6.
2. Azhar EI, Hashem AM, El-Kafrawy SA, et al. Detection of the Middle East respiratory syndrome coronavirus genome in an air sample originating from a camel barn owned by an infected patient. mBio **2014**; 5:e01450-14.
3. Booth TF, Kournikakis B, Bastien N, et al. Detection of airborne severe acute respiratory syndrome (SARS) coronavirus and environmental contamination in SARS outbreak units. J Infect Dis **2005**; 191:1472–7.
4. Xiao WJ, Wang ML, Wei W, et al. Detection of SARS-CoV and RNA on aerosol samples from SARS-patients admitted to hospital [in Chinese]. Zhonghua Liu Xing Bing Xue Za Zhi **2004**; 25:882–5.
5. Kim SH, Chang SY, Sung M, et al. Extensive viable Middle East respiratory syndrome (MERS) coronavirus contamination in air and surrounding environment in MERS isolation wards. Clin Infect Dis **2016**; 63:363–9.
6. Guo Z, Wang Z, Zhang S, et al. Aerosol and surface distribution of severe acute respiratory syndrome coronavirus 2 in hospital wards, Wuhan, China, 2020 [published online ahead of print 10 April 2020]. Emerg Infect Dis doi: 10.3201/eid2607.200885.
7. Liu Y, Ning Z, Chen Y, et al. Aerodynamic analysis of SARS-CoV-2 in two Wuhan hospitals [published online ahead of print 27 April 2020]. Nature doi: 10.1038/s41586-020-2271-3.
8. Chia PY, Coleman KK, Tan YK, et al. Detection of air and surface contamination by SARS-CoV-2 in hospital rooms of infected patients. Nat Commun **2020**; 11:1–7. Available from https://www.nature.com/articles/s41467-020-16670-2.
9. Lindsley WG, Pearce TA, Hudnall JB, et al. Quantity and size distribution of cough-generated aerosol particles produced by influenza patients during and after illness. J Occup Environ Hyg **2012**; 9:443–9.
10. Morawska L, Johnson G, Ristovski Z, et al. Size distribution and sites of origin of droplets expelled from the human respiratory tract during expiratory activities. J Aerosol Sci **2009**; 40:256–69.
11. Leung NH, Chu DK, Shiu EY, et al. Respiratory virus shedding in exhaled breath and efficacy of face masks. Nat Med **2020**; 26:676–80.
12. Pan Y, Zhang D, Yang P, Poon LLM, Wang Q. Viral load of SARS-CoV-2 in clinical samples. Lancet Infect Dis **2020**; 20:411–2.
13. Zou L, Ruan F, Huang M, et al. SARS-CoV-2 viral load in upper respiratory specimens of infected patients. N Engl J Med **2020**; 382:1177–9.
14. Wang W, Xu Y, Gao R, et al. Detection of SARS-CoV-2 in different types of clinical specimens. JAMA **2020**; 323:1843–4.
15. Bischoff WE, Swett K, Leng I, Peters TR. Exposure to influenza virus aerosols during routine patient care. J Infect Dis **2013**; 207:1037–46.
16. Heinsohn P, Jewett DL. Exposure to blood-containing aerosols in the operating room: a preliminary study. Am Ind Hyg Assoc J **1993**; 54:446–53.
17. van Doremalen N, Bushmaker T, Morris DH, et al. Aerosol and surface stability of SARS-CoV-2 as compared with SARS-CoV-1. N Engl J Med **2020**; 382:1564–7.
18. Ijaz MK, Brunner AH, Sattar SA, Nair RC, Johnson-Lussenburg CM. Survival characteristics of airborne human coronavirus 229E. J Gen Virol **1985**; 66:2743–8.
19. Pyankov OV, Bodnev SA, Pyankova OG, Agranovski IE. Survival of aerosolized coronavirus in the ambient air. J Aerosol Sci **2018**; 115:158–63.
20. Berendt RF, Dorsey EL. Effect of simulated solar radiation and sodium fluorescein on the recovery of Venezuelan equine encephalomyelitis virus from aerosols. Appl Microbiol **1971**; 21:447–50.
21. Schuit M, Gardner S, Wood S, et al. The influence of simulated sunlight on the inactivation of influenza virus in aerosols. J Infect Dis **2020**; 221:372–8.
22. Van Doremalen N, Bushmaker T, Munster V. Stability of Middle East respiratory syndrome coronavirus (MERS-CoV) under different environmental conditions. Eurosurveillance **2013**; 18:20590.
23. Harper GJ. Airborne micro-organisms: survival tests with four viruses. J Hyg (Lond) **1961**; 59:479–86.
24. Zhao Y, Aarnink AJ, Dijkman R, Fabri T, de Jong MC, Groot Koerkamp PW. Effects of temperature, relative humidity, absolute humidity, and evaporation potential on survival of airborne Gumboro vaccine virus. Appl Environ Microbiol **2012**; 78:1048–54.

25. ASTM International. E2721-16 Standard practice for evaluation of effectiveness of decontamination procedures for surfaces when challenged with droplets containing human pathogenic viruses. West Conshohocken, PA: ASTM International, **2016**.
26. Kärber G. Beitrag zur kollektiven Behandlung pharmakologischer Reihenversuche. Naunyn-Schmiedebergs Arch Exp Pathol Pharmakol **1931**; 162:480–3.
27. Spearman C. The method of "right and wrong cases"("constant stimuli") without Gauss's formulae. Br J Psychol 1904–1920 **1908**; 2:227–42.
28. Milton DK, Fabian MP, Cowling BJ, Grantham ML, McDevitt JJ. Influenza virus aerosols in human exhaled breath: particle size, culturability, and effect of surgical masks. PLoS Pathog **2013**; 9: e1003205.
29. Lindsley WG, Blachere FM, Thewlis RE, et al. Measurements of airborne influenza virus in aerosol particles from human coughs. PloS One **2010**; 5:e15100.
30. Ehresmann DW, Hatch MT. Effect of relative humidity on the survival of airborne unicellular algae. Appl Environ Microbiol **1975**; 29:352–7.
31. Goldberg L, Watkins H, Boerke E, Chatigny M. The use of a rotating drum for the study of aerosols over extended periods of time. Am J Hyg **1958**; 68:85–93.
32. Webb S. Factors affecting the viability of air-borne bacteria: I. Bacteria aerosolized from distilled water. Can J Microbiol **1959**; 5:649–69.
33. Turgeon N, Michel K, Ha T-L, Robine E, Moineau S, Duchaine C. Resistance of aerosolized bacterial viruses to four germicidal products. PloS One **2016**; 11:e0168815.
34. Walker CM, Ko G. Effect of ultraviolet germicidal irradiation on viral aerosols. Environ Sci Technol **2007**; 41:5460–5.
35. Donaldson AI. The influence of relative humidity on the aerosol stability of different strains of foot-and-mouth disease virus suspended in saliva. J Gen Virol **1972**; 15: 25–33.
36. Mitchell CA, Guerin LF. Influenza A of human, swine, equine and avian origin: comparison of survival in aerosol form. Can J Comp Med **1972**; 36:9–11.
37. Piercy TJ, Smither SJ, Steward JA, Eastaugh L, Lever MS. The survival of filoviruses in liquids, on solid substrates and in a dynamic aerosol. J Appl Microbiol **2010**; 109:1531–9.
38. Mitchell CA, Guerin LF, Robillard J. Decay of influenza A viruses of human and avian origin. Can J Comp Med **1968**; 32:544–6.
39. Benbough J. The effect of relative humidity on the survival of airborne Semliki Forest virus. J Gen Virol **1969**; 4:473–7.
40. Kormuth KA, Lin K, Prussin AJ, et al. Influenza virus infectivity is retained in aerosols and droplets independent of relative humidity. J Infect Dis **2018**; 218:739–47.
41. Zuo Z, Kuehn TH, Bekele AZ, et al. Survival of airborne MS2 bacteriophage generated from human saliva, artificial saliva, and cell culture medium. Appl Environ Microbiol **2014**; 80:2796–803.